



UvA-DARE (Digital Academic Repository)

The X-ray spectral properties of very-faint persistent neutron star X-ray binaries

Armas Padilla, M.; Degenaar, N.; Wijnands, R.

DOI

[10.1093/mnras/stt1114](https://doi.org/10.1093/mnras/stt1114)

Publication date

2013

Document Version

Final published version

Published in

Monthly Notices of the Royal Astronomical Society

[Link to publication](#)

Citation for published version (APA):

Armas Padilla, M., Degenaar, N., & Wijnands, R. (2013). The X-ray spectral properties of very-faint persistent neutron star X-ray binaries. *Monthly Notices of the Royal Astronomical Society*, 434(2), 1586-1592. <https://doi.org/10.1093/mnras/stt1114>

General rights

It is not permitted to download or to forward/distribute the text or part of it without the consent of the author(s) and/or copyright holder(s), other than for strictly personal, individual use, unless the work is under an open content license (like Creative Commons).

Disclaimer/Complaints regulations

If you believe that digital publication of certain material infringes any of your rights or (privacy) interests, please let the Library know, stating your reasons. In case of a legitimate complaint, the Library will make the material inaccessible and/or remove it from the website. Please Ask the Library: <https://uba.uva.nl/en/contact>, or a letter to: Library of the University of Amsterdam, Secretariat, Singel 425, 1012 WP Amsterdam, The Netherlands. You will be contacted as soon as possible.



The X-ray spectral properties of very-faint persistent neutron star X-ray binaries

M. Armas Padilla,¹* N. Degenaar²† and R. Wijnands¹

¹Astronomical Institute ‘Anton Pannekoek’, University of Amsterdam, Postbus 94249, NL-1090 GE Amsterdam, the Netherlands

²Department of Astronomy, University of Michigan, 500 Church Street, Ann Arbor, MI 48109, USA

Accepted 2013 June 18. Received 2013 June 13; in original form 2013 March 13

ABSTRACT

AX J1754.2–2754, 1RXS J171824.2–402934 and 1RXH J173523.7–354013 are three persistent neutron star low-mass X-ray binaries that display a 2–10 keV accretion luminosity L_X of only $(1–10) \times 10^{34} \text{ erg s}^{-1}$ (i.e. only $\simeq 0.005–0.05$ per cent of the Eddington limit). The phenomenology of accreting neutron stars which accrete at such low accretion rates is not yet well known and the reason why they have such low accretion rates is also not clear. Therefore, we have obtained *XMM–Newton* data of these three sources and here we report our analysis of the high-quality X-ray spectra we have obtained for them. We find that AX J1754.2–2754 has $L_X \sim 10^{35} \text{ erg s}^{-1}$, while the other two have X-ray luminosities about an order of magnitude lower. However, all sources have a similar, relatively soft, spectrum with a photon index of 2.3–2.5, when the spectrum is fitted with an absorbed power-law model. This model fits the data of AX J1754.2–2754 adequately, but it cannot fit the data obtained for 1RXS J171824.2–402934 and 1RXH J173523.7–354013. For those sources, a clear soft thermal component is needed to fit their spectra. This soft component contributes 40–50 per cent to the 0.5–10 keV flux of the sources. The presence of this soft component might be the reason why the spectra of these two sources are soft. When including this additional spectral component, the power-law photon indices are significantly lower. It can be excluded that a similar component with similar contributions to the 2–10 keV X-ray flux is present for AX J1754.2–2754, indicating that the soft spectrum of this source is mostly due to the fact that the power-law component itself is not hard. We note that we cannot exclude that a weaker soft component is present in the spectrum of this source which only contributes up to ~ 25 per cent to the 0.5–10 keV X-ray flux. We discuss our results in the context of what is known of accreting neutron stars at very low accretion rate.

Key words: accretion, accretion discs – stars: neutron – stars: individual: AX J1754.2–2754 – stars: individual: 1RXS J171824.2–402934 – stars: individual: 1RXH J173523.7–354013 – X-rays: binaries.

1 INTRODUCTION

Low-mass X-ray binaries (LMXBs) are systems in which a neutron star (NS) or black hole accretes material from a Roche-lobe filling companion star that typically is less massive than the accretor. Transient X-ray binaries alternate long-lived quiescent periods (typically years to decades) during which the systems are extremely faint in the X-rays ($< 10^{33} \text{ erg s}^{-1}$; during which no or hardly any accretion occurs) with short-lived (weeks to months) accretion out-

burst episodes during which the X-ray luminosity increases several orders of magnitude. It is thought that those outbursts are powered by a similar large increase in the mass accretion rate on to the central compact object. On the other hand, the persistent systems are continuously accreting and therefore their X-ray luminosities are always order of magnitudes higher than the X-ray luminosities in quiescence. Although large fluctuations in their X-ray brightness are commonly observed (sometimes fluctuations of more than a factor of 10), they do not become as faint as the X-ray transients in quiescence.

Very faint X-ray binaries (VFXBs) are those systems that show maximum 2–10 keV X-ray luminosities of only $\sim 10^{34–36} \text{ erg s}^{-1}$ (Wijnands et al. 2006). These sub-luminous sources are interesting

* E-mail: m.armaspadilla@uva.nl

† Hubble fellow.

because they probe a relatively unexplored mass-accretion regime and can therefore provide valuable input for accretion physics (e.g. Armas Padilla et al. 2011, 2013), binary evolution models (e.g. King & Wijnands 2006; Degenaar & Wijnands 2009, 2010; Maccarone & Patruno 2013) and the theory of nuclear burning on the surface of accreting NS (e.g. Cooper & Narayan 2007; Peng, Brown & Truran 2007; Degenaar et al. 2010).

At the time of writing, only a handful of VFXBs persistently accreting at such very low accretion rates are known (e.g. in't Zand, Cornelisse & Méndez 2005; in't Zand, Jonker & Markwardt 2007; Degenaar et al. 2010, 2012a; Degenaar, Altamirano & Wijnands 2012c). The very faint persistent systems for which the accretor has conclusively been identified harbour an NS because they exhibited a type I burst. However, the fact that we do not know any black hole system is very likely a selection effect because without observing type I bursts or pulsations, the nature of the accretor is very difficult to identify. The reason why those sources exhibit such faint accretion luminosities remains unclear. It has been proposed that persistent VFXBs could be ultracompact X-ray binaries (UCXBs; King 2000). These are systems that are thought to harbour an hydrogen-poor companion star in a very small orbit around the accretor with an orbital period $P \lesssim 80\text{--}90$ min (e.g. Nelson, Rappaport & Joss 1986; Nelemans & Jonker 2010). However, although a very short orbital period could justify the low luminosity for some sources, it cannot explain all persistent VFXBs (Degenaar et al. 2010, see section 1.3).

In this work we report on the analysis of high-quality *XMM-Newton* spectra of three persistent sub-luminous NS LMXBs: AX J1754.2–2754, 1RXS J171824.2–402934 and 1RXH J173523.7–354013.

1.1 AX J1754.2–2754

AX J1754.2–2754 is a faint X-ray source that was discovered with *ASCA* in 1999 (Sakano et al. 2002). The nature of the source remained unknown until *INTEGRAL* detected a type I X-ray burst in 2005, which unambiguously identified it as an accreting NS in an LMXB (Chelovekov & Grebenev 2007). Assuming that the peak X-ray burst was equal to or lower than the Eddington luminosity, the source distance was estimated to be $D \lesssim 6.6$ kpc for a hydrogen atmosphere of the NS, and $D \lesssim 9.2$ kpc for a helium atmosphere.

The source has been detected at a 2–10 keV luminosity of $L_X \simeq 10^{35}$ erg s^{−1} every time an X-ray satellite is pointed at it (Del Santo et al. 2007b; Krivonos et al. 2007; Bassa et al. 2008; Jonker & Keek 2008; Degenaar et al. 2012a; Maccarone et al. 2012), except for a brief episode in 2008, when *Chandra* did not detect the source with an upper limit of $L_X \simeq 5 \times 10^{32}$ erg s^{−1} (Bassa et al. 2008). The non-detection might have been caused by an eclipse, although this scenario is not very likely (Jonker & Keek 2008). Instead, it is more likely that the source was inactive for a brief period, which must have been rather short (<1 yr; Degenaar et al. 2012a). This inactive period would indicate that the source is a transient but its unusual short inactive phase compared to the very long active phase makes this system quite an oddball among the transients. Since the source is active for such an extended period of time, we expect that the accretion flow geometry in this source is likely to be very similar to that present in the persistent sources and therefore we treat the source as a persistent source in the remainder of this paper.

The source has a low absolute optical magnitude, which has led to the suggestion that it might be an UCXB (Bassa et al. 2008). However, no orbital period is known for this source so its classification as a UCXB is still uncertain.

Analysis of a series of *Swift* observations suggests that the X-ray spectrum of AX J1754.2–2754 is strongly absorbed (with a column density $N_H \simeq 2.1 \times 10^{22}$ cm^{−2}) and relatively soft (with a photon index $\Gamma \simeq 2.7\text{--}3.6$; Del Santo et al. 2008; Degenaar et al. 2012a). The *Swift* spectral data could be adequately fitted with a single power-law model, but the data quality was such that a multiple component spectrum could not be excluded.

1.2 1RXS J171824.2–402934

1RXS J171824.2–402934 was discovered with *ROSAT* in 1990 and identified as an NS LMXB when a type I X-ray burst was detected with *BeppoSAX* in 1997 (Kaptein et al. 2000). The X-ray burst showed evidence for photospheric radius expansion. Assuming Eddington-limited emission during the burst peak places the source at an upper limit distance of $D \lesssim 6.5$ kpc for an H-rich photosphere, or $D \lesssim 9$ kpc if a helium atmosphere is assumed (in't Zand et al. 2005). The source is persistently detected at a 2–10 keV persistent luminosity of $L_X \simeq (5\text{--}10) \times 10^{34}$ erg s^{−1} (in't Zand et al. 2005, 2009). A *Chandra* observation showed that the X-ray spectrum of the source can be described by a power-law model with $N_H \simeq 1 \times 10^{22}$ cm^{−2} and $\Gamma \simeq 2.1\text{--}2.4$ (in't Zand et al. 2005, 2009).

1.3 1RXH J173523.7–354013

1RXH J173523.7–354013 is a faint X-ray source that was discovered with *ROSAT* in 1990. It was identified as an NS LMXB when *Swift* detected a type I X-ray burst in 2008 (Israel et al. 2008; Degenaar et al. 2010). From the analysis of the X-ray burst a source distance of $D \lesssim 9.5$ kpc is suggested, assuming that the peak flux was equal to or lower than the Eddington luminosity and a helium atmosphere for the NS. When an H-rich atmosphere is assumed, the distance lowers to $D \lesssim 6.2$ kpc. Its X-ray spectrum can be described by an absorbed power law with $N_H \simeq 9 \times 10^{21}$ cm^{−2} and $\Gamma \simeq 2.3$. The source is always detected at a 2–10 keV luminosity of $L_X \simeq 10^{35}$ erg s^{−1} (Degenaar et al. 2010).

1RXH J173523.7–354013 has an optical/IR counterpart with observed magnitudes of $V \simeq 21.2$, $R \simeq 18.8$, $J \simeq 15.4$, $H \simeq 14.3$ and $K \simeq 13.8$ mag. Optical spectroscopy revealed a strong H α emission line, which suggests that the NS is accreting H-rich material (Degenaar et al. 2010) and therefore the system cannot be a UCXB.

2 OBSERVATIONS AND DATA ANALYSIS

In order to investigate the spectral properties of VFXBs in greater detail than previous studies, we acquired *XMM-Newton* observations of the three VFXBs discussed in Section 1 (Table 1 shows a log of the observations). We use the data obtained with the European Photon Imaging Cameras, which consists of two MOS detectors (Turner et al. 2001) and one PN camera (Strüder et al. 2001). During all three observations the MOS cameras were operated in imaging mode using the small window for 1RXH J173523.7–354013 and the full-frame window for AX J1754.2–2754 and 1RXS J171824.2–402934, whereas the PN was set in timing mode for the three observations. The timing mode was used to allow searches for the expected millisecond X-ray pulsations in these sources arising from a possible fast rotating NS in them (e.g. Wijnands 2008). However, no pulsations were found (see Patruno 2010 for the results on 1RXS J171824.2–402934; a full description will be published elsewhere). Given the faintness of our sources and the calibration uncertainties in the soft part of the spectrum in the PN data in timing

Table 1. Target list and *XMM-Newton* observation log.

Source	Observation ID	Date (yyyy-mm-dd)	Exposure time (ks)	Net exposure time ^a (ks)	Net count rate (counts s ⁻¹)
AX J1754.2–2754	0651450201	2011-03-17	47.5	42	0.54
1RXS J171824.2–402934	0605160101	2010-03-14	76.8	70	0.25
1RXH J173523.7–354013	0606200101	2010-03-20	40.0	28	0.17

^aNet exposure time after removing episodes of background flaring.

mode (see the *XMM-Newton* calibration technical note XMM-SOC-CALTN-0083;¹ see also, e.g., Done & Diaz Trigo 2010), we have excluded the PN spectra from our analysis.

The data analysis and reduction were carried out with the Science Analysis Software (*SAS*, v. 12.0.1) to obtain calibrated event lists and scientific products. The observations were affected by episodes of high background. To eliminate these background flaring periods, we excluded data with count rates larger than 0.35 counts s⁻¹ at energies > 10 keV. The count rates of the three observations were lower than 0.55 counts s⁻¹ (see Table 1), while the pile starts to be an issue at count rates above ~0.7 counts s⁻¹ (see the *XMM-Newton* users' handbook²). Therefore, our sources are not bright enough for pile-up to become considerable and there was not need to correct for that. We extracted the MOS source events using a circular region with a radius of ~950, ~1000 and ~700 pixels for AX J1754.2–2754, 1RXS J171824.2–402934 and 1RXH J173523.7–354013, respectively. The background events were extracted from circles with the same sizes and were located on nearby source-free regions. We generated the light curves and the spectra, as well as the associated response matrix files (RMFs) and ancillary response files (ARFs) using the standard analysis threads.³ The spectral data were grouped to contain a minimum of 25 photons per bin and rebinned to oversample the full width at half-maximum of the energy resolution by a factor of 3.

For each observation, we fitted simultaneously the 0.5–10 keV spectra of the two MOS cameras using *XSPEC* (v. 12.8; Arnaud 1996). The model parameters were tied between the two detectors. We added a constant factor (CONSTANT) to the spectral models with a value fixed to one for MOS1 camera but we allowed it to vary freely for MOS2 in order to account for cross-calibration uncertainties. We included the photoelectric absorption component (PHABS) to account for the interstellar absorption assuming the cross-sections of Verner et al. (1996) and the abundances of Wilms, Allen & McCray (2000).

3 RESULTS

We used six different models to fit our spectra. First, we used a simple power law (POWERLAW) affected by photoelectric absorption, and then we added a soft component, using either a blackbody (BBODYRAD) or an accretion disc model consisting of multiple blackbody components (DISKBB; Makishima et al. 1986). In order to investigate the effects of our choice of model for the hard component on our results, we repeated the fits replacing the POWERLAW with a thermally Comptonized continuum model (NTHCOMP; Zdziarski, Johnson & Magdziarz 1996; Życki, Done & Smith 1999). In the fits with the two component models,

we tied the seed photon temperature (low-energy rollover; kT_{bb}) to the blackbody temperature when using BBODYRAD model, and to the temperature at inner disc radius when using the DISKBB model. The obtained photon index and temperatures are, within the uncertainties, compatible with the values obtained when using the POWERLAW, although we note that for AX J1754.2–2754 the fit using the NTHCOMP is unstable inhibiting us to correctly determine the errors. For simplicity, in the main body of this paper, we only discuss the POWERLAW results, which are summarized in Table 2. The uncertainties on the spectral parameters are at 90 per cent confidence level and the flux errors have been calculated following the procedure presented by Wijnands et al. (2004). All three NS exhibited very energetic thermonuclear X-ray bursts that were likely caused by the ignition of a layer of pure He. We therefore adopt the distances that were inferred by assuming pure He bursts when calculating luminosities and blackbody/DISKBB emitting radii. These are 9.2 kpc for AX J1754.2–2754 (Chelovekov & Grebenev 2007), 9 kpc for 1RXS J171824.2–402934 (in't Zand et al. 2005) and 9.5 kpc for 1RXH J173523.7–354013 (Degenaar et al. 2010).

3.1 AX J1754.2–2754

The spectrum of AX J1754.2–2754 can be well described by a single power-law model [$\chi^2_{\nu} \sim 0.96$ for 279 degrees of freedom (dof); Fig. 1]. The N_{H} obtained is $\sim 2.9 \times 10^{22}$ cm⁻². The X-ray spectra are quite soft: the obtained photon index is $\Gamma = 2.5$, which is (within the uncertainties) in agreement with the value ($\Gamma = 2.7 \pm 0.2$) obtained by Degenaar et al. (2012a) in their analysis of *Swift* data of the source (however, see Del Santo et al. 2008 who found a higher value; $\Gamma = 3.6 \pm 0.7$). Adding a soft spectral does not improve the fit significantly ($\chi^2_{\nu} \sim 0.93$ for 277 dof). When we do add a soft component to the power-law model, the photon index becomes $\Gamma \sim 2.3$ or $\Gamma \sim 2$, and the temperatures obtained are 0.53 or 0.74 keV for the blackbody and DISKBB, respectively. The fractional contribution of the thermal component to the total unabsorbed 0.5–10 keV and 2–10 keV fluxes are almost the same, with a higher contribution if we use the DISKBB (~26 per cent) than using the BBODYRAD (~8 per cent). For all fits the unabsorbed 2–10 keV flux obtained is $\sim 9.5 \times 10^{-12}$ erg cm⁻² s⁻¹ which corresponds to a luminosity of $\sim 1 \times 10^{35}$ erg s⁻¹ assuming a distance of 9.2 kpc.

3.2 1RXS J171824.2–402934

The spectrum of 1RXS J171824.2–402934 is not well described by a single power-law model ($\chi^2_{\nu} \sim 2.5$ for 277 dof; see the residuals shown in Fig. 1) and it is required to add an additional component (for which we use a soft, thermal component) to get an acceptable fit ($\chi^2_{\nu} \sim 1.03$ for 275 dof; Fig. 1). The obtained column density is $\sim 2 \times 10^{22}$ cm⁻² and the photon index $\Gamma \sim 1.5$, which is considerably harder than the $\Gamma = 2.3$ obtained with the simple power-law model. The temperature of the blackbody (DISKBB) component

¹ <http://xmm.esac.esa.int/>

² http://xmm.esac.esa.int/external/xmm_user_support/documentation/uhb_2.1/XMM_UHB.html

³ <http://xmm.esac.esa.int/sas/current/documentation/threads/>

Table 2. Results from fitting the spectral data.

Source	N_{H} (10^{22} cm^{-2})	Γ	kT (keV)	$R_{\text{bb/in}}$ (km)	T_{ir} (per cent)	$F_{\text{X,abs}}$ ($10^{-12} \text{ erg cm}^{-2} \text{ s}^{-1}$)	$F_{\text{X,unabs}}$ ($10^{-12} \text{ erg cm}^{-2} \text{ s}^{-1}$)	L_{X} ($10^{34} \text{ erg s}^{-1}$)	T_{ir} (per cent)	$F_{\text{X,abs}}$ ($10^{-12} \text{ erg cm}^{-2} \text{ s}^{-1}$)	$F_{\text{X,unabs}}$ ($10^{-12} \text{ erg cm}^{-2} \text{ s}^{-1}$)	L_{X} ($10^{34} \text{ erg s}^{-1}$)	χ^2_{ν} (dof)
PHABS*(POWERLAW)													
AX J1754	2.93 ± 0.06	2.51 ± 0.03	—	—	—	8.81 ± 0.06	27.0 ± 0.8	27.4 ± 0.8	—	7.70 ± 0.06	9.55 ± 0.02	9.67 ± 0.02	$0.96 (279)$
1RXS J1718	1.78 ± 0.04	2.33 ± 0.04	—	—	—	3.59 ± 0.04	8.0 ± 0.2	7.8 ± 0.1	—	2.95 ± 0.04	3.33 ± 0.03	3.23 ± 0.02	$2.54 (277)$
1RXH J1735	1.43 ± 0.07	2.45 ± 0.07	—	—	—	2.29 ± 0.05	5.2 ± 0.3	5.6 ± 0.3	—	1.76 ± 0.05	1.93 ± 0.05	2.08 ± 0.05	$1.92 (186)$
PHABS*(POWERLAW+BBODYRAD)													
AX J1754	2.7 ± 0.2	2.3 ± 0.2	0.53 ± 0.04	1.4 ± 1.2	8.4	8.90 ± 0.08	22 ± 3	22 ± 3	9	7.79 ± 0.09	9.4 ± 0.06	9.57 ± 0.06	$0.93 (277)$
1RXS J1718	1.9 ± 0.1	1.6 ± 0.1	0.31 ± 0.02	$5.1^{+0.5}_{-0.7}$	37.2	4.01 ± 0.05	7.8 ± 0.5	7.6 ± 0.2	9.4	3.34 ± 0.05	3.75 ± 0.04	3.63 ± 0.02	$1.03 (275)$
1RXH J1735	1.4 ± 0.1	1.4 ± 0.2	0.30 ± 0.02	$4.8^{+0.6}_{-1.1}$	42.2	2.66 ± 0.07	4.8 ± 0.5	5.2 ± 0.5	10	2.10 ± 0.06	2.29 ± 0.06	2.48 ± 0.06	$0.97 (184)$
PHABS*(POWERLAW+DISKBB)													
AX J1754	2.6 ± 0.2	2.0 ± 0.3	0.74 ± 0.06	$0.9^{+0.9}_{-0.7}$	25.9	9.0 ± 0.1	20 ± 5	20 ± 5	19.5	7.9 ± 0.1	9.45 ± 0.07	9.57 ± 0.07	$0.92 (277)$
1RXS J1718	2.1 ± 0.1	1.5 ± 0.1	0.39 ± 0.03	$3.4^{+0.6}_{-0.9}$	49.1	4.02 ± 0.05	9.4 ± 0.7	9.1 ± 0.4	11.2	3.35 ± 0.05	3.81 ± 0.04	3.69 ± 0.02	$1.03 (275)$
1RXH J1735	1.7 ± 0.1	1.4 ± 0.2	0.38 ± 0.03	$3.2^{+0.8}_{-1.5}$	53.8	2.66 ± 0.07	5.9 ± 0.7	6.4 ± 0.7	11.6	2.11 ± 0.07	2.33 ± 0.06	2.52 ± 0.06	$0.97 (184)$

Note. Quoted errors represent 90 per cent confidence levels. The fifth and ninth column reflects the fractional contribution of the thermal component to the total unabsorbed 0.5–10 keV and 2–10 keV flux, respectively. $F_{\text{X,abs}}$ and $F_{\text{X,unabs}}$ represent the absorbed and unabsorbed fluxes, respectively. The luminosity L_{X} , source radius (R_{bb}) and apparent inner disc radius (R_{in}) were calculated adopting distances of 9.2, 9, and 9.5 kpc for AX J1754.2–2754, 1RXS J171824.2–402934 and 1RXH J173523.7–354013, respectively. Also we assumed a disc angle $\theta = 0$ to calculate R_{in} .

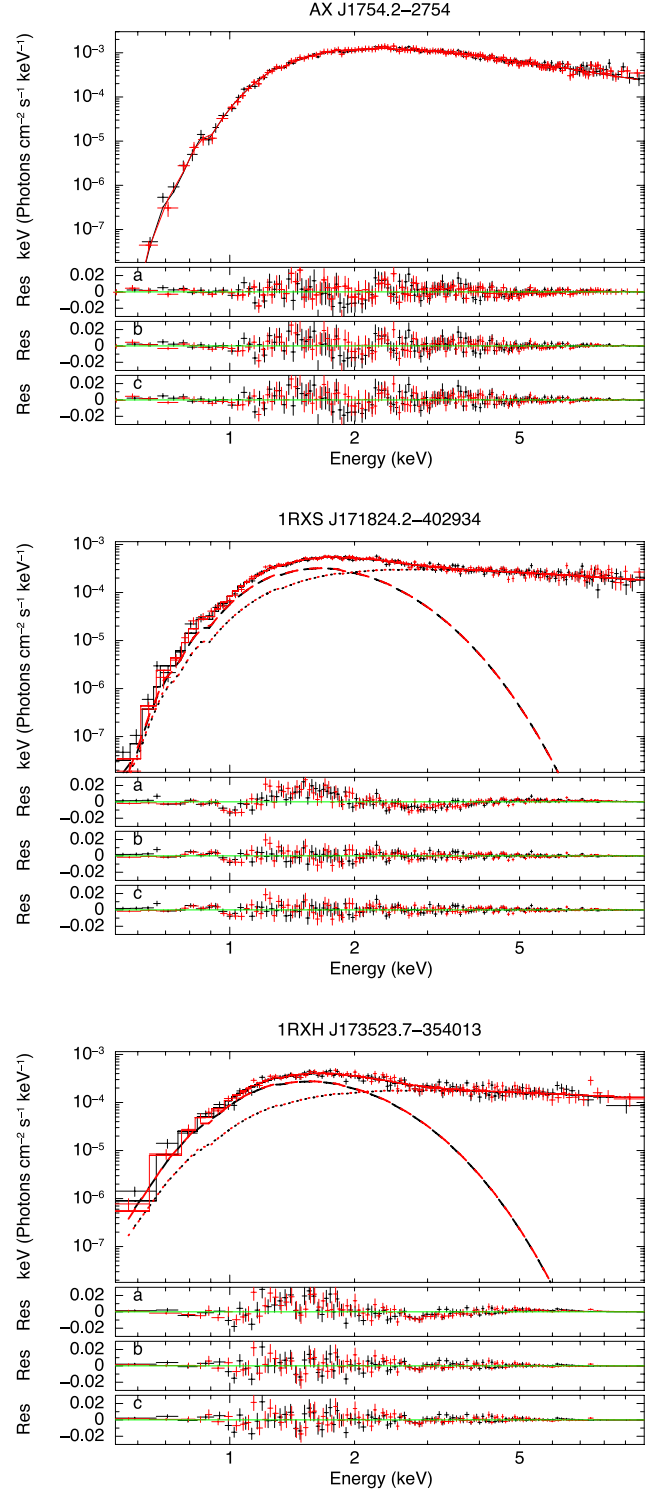


Figure 1. MOS1 (black) and MOS2 (red) spectra. The solid lines represent the best fit for a POWERLAW model in the case of AX J1754.2–2754 (top panel), and a combined POWERLAW (dotted lines) and BBODYRAD (dashes) model for 1RXS J171824.2–402934 (middle panel) and 1RXH J173523.7–354013 (bottom panel). In the sub-panels the residuals are plotted when fitting with (a) POWERLAW, (b) POWERLAW+BBODYRAD and (c) POWERLAW+DISKBB models

is 0.31 keV (0.39 keV), which contributes 37 per cent (49 per cent) in the total 0.5–10 keV unabsorbed flux and only 9 per cent (11 per cent) in the total 2–10 keV one. The unabsorbed flux is $\sim 4 \times 10^{-12}$ erg cm $^{-2}$ s $^{-1}$ (2–10 keV) when we use the BBODYRAD component. Assuming a distance of 9 kpc, the corresponding luminosity is $\sim 3.6 \times 10^{34}$ erg s $^{-1}$. The unabsorbed values are slightly higher when using the DISKBB model.

3.3 1RXH J173523.7–354013

1RXH J173523.7–354013 has similar spectral characteristics as 1RXS J171824.2–402934. It also needs a two-component model to obtain a good fit ($\chi^2_{\nu} = 0.97$ for 184 dof for a two-component model versus $\chi^2_{\nu} = 1.92$ with 186 dof for a single power-law model; Fig. 1). The thermal component contributes about half of the total 0.5–10 keV unabsorbed flux while only ~ 10 per cent in the 2–10 keV energy range. The parameters obtained are $N_{\text{H}} \sim 1.5 \times 10^{22}$ cm $^{-2}$, a photon index of $\Gamma \sim 1.4$ and a temperature of 0.3 keV for the BBODYRAD (slightly higher if the DISKBB component is used; 0.4 keV). The unabsorbed 2–10 keV flux is $\sim 2.3 \times 10^{-12}$ erg cm $^{-2}$ s $^{-1}$ which translates to a luminosity of $\sim 2.5 \times 10^{34}$ erg s $^{-1}$ for a distance of 9.5 kpc.

4 DISCUSSION

We have presented the spectral analysis of our high-quality *XMM-Newton* data of the persistent NS LMXBs AX J1754.2–2754, 1RXS J171824.2–402934 and 1RXH J173523.7–354013. Their 2–10 keV X-ray luminosities are $L_{\text{X}} \simeq (2\text{--}10) \times 10^{34}$ erg s $^{-1}$, which implies that these NS are accreting at $\simeq 0.01\text{--}0.05$ per cent of the Eddington rate (assuming an Eddington luminosity of $L_{\text{EDD}} = 3.8 \times 10^{38}$ erg s $^{-1}$; Kuulkers et al. 2003).

Previous *Swift* and *Chandra* observations of 1RXS J171824.2–402934 could be satisfactorily modelled with an absorbed power-law model ($\Gamma \simeq 2.1\text{--}2.4$; in't Zand et al. 2005, 2009). Fitting our *XMM-Newton* data of the source with a single power-law model gives a similar photon index. However, due to the quality of our data, it has now been possible to determine that the spectrum can be better described by a two-component model, consisting of a power-law plus a soft component. This soft component could satisfactorily be modelled with either a blackbody or a disc blackbody model. Such a two-component model results in a significantly harder photon index ($\Gamma \sim 1.5$) compared to the single power-law model. The temperature of the soft component is $\sim 0.3\text{--}0.4$ keV.

We obtained similar results for 1RXH J173523.7–354013. The values obtained with the absorbed power-law model are in agreement with the ones reported by Degenaar et al. (2010) using *Swift* data (they obtained a photon index of $\Gamma \sim 2.3$ compared to our 2.5). However, the *XMM-Newton* spectral analysis shows the presence of a thermal component with a temperature $\sim 0.3\text{--}0.4$ keV and consequently, the photon index has (similarly to 1RXS J171824.2–402934) a lower value ($\Gamma \sim 1.4$). AX J1754.2–2754 is the only one of the three sources that is well described by only a simple absorbed power-law model and the addition of a soft spectral component did not improve the fit. This is consistent with the results obtained by Degenaar et al. (2012a) and Del Santo et al. (2008) who analysed *Swift* observations obtained from this source. AX J1754.2–2754 has the highest column density of the three sources ($N_{\text{H}} \sim 2.9 \times 10^{22}$ cm $^{-2}$) but we determined that this high column density could not explain why we do not

see a soft component in its spectrum with similar strength as what we observed for the other two sources (see below). Another difference is that AX J1754.2–2754 is the most luminous of the three sources ($L_{\text{X}} \sim 10^{35}$ erg s $^{-1}$ for AX J1754.2–2754 compared with the $L_{\text{X}} \sim 3\text{--}4 \times 10^{34}$ erg s $^{-1}$ for the other two sources; 2–10 keV).

One question is why the soft component is detected in some sources and not in others. The data quality of our three sources is similar; in fact the AX J1754.2–2754 data are slightly better. Hence, the spectral differences are not due to differences in the quality of the data. One possibility is the difference in the absorption by the interstellar medium along the line of sight towards the sources. We have carried out simulations in order to quantify the effect of the high N_{H} on our ability to detect a soft component in the spectra. Using XSPEC we simulated a variety of spectra using the RMFs and ARFs for the MOS cameras, an exposure time of 30 ks and the parameters obtained for 1RXS J171824.2–402934 and 1RXH J173523.7–354013 but with an N_{H} up to 3×10^{22} cm $^{-2}$. We found that despite that its contribution to the total absorbed flux is lower, the thermal component is still clearly detectable (albeit at lower significance) if its contribution to the total unabsorbed flux is similar as what has been observed for 1RXS J171824.2–402934 and 1RXH J173523.7–354013 ($\sim 40\text{--}50$ per cent in the 0.5–10 keV energy range). Therefore, the reason for the spectral differences cannot be explained by differences in absorption columns alone and must be intrinsic to the sources.

We have searched the literature for information about what is known about the spectral properties of other persistent VFXBs. The NS LMXB XMMU J174716.1–281048 is such source, although strictly speaking it is a quasi-persistent LMXB because before 2001 it could not be detected (but has been detected ever since; Sidoli & Mereghetti 2003; Del Santo et al. 2007a; Degenaar, Wijnands & Kaur 2011). Its 2–10 keV X-ray luminosity is $L_{\text{X}} \sim 5 \times 10^{34}$ erg s $^{-1}$ (Del Santo et al. 2007a). Its *XMM-Newton* spectra were well described with an absorbed power-law model, with a photon index of $\Gamma \sim 2$ but its column density is very high with a value of $N_{\text{H}} \sim 9 \times 10^{22}$ cm $^{-2}$ which could easily absorb the flux from even a rather strong thermal component. We note that, as discussed above, this cannot be the reason why we do not see a thermal component in AX J1754.2–2754 because the column density of that source is significantly lower than what is observed for XMMU J174716.1–281048. Therefore the absence of a soft thermal component in AX J1754.2–2754 is likely to be intrinsic for this source. The unclassified persistent source AX J1538.3–5541 reaches similar luminosities and its spectrum can be described with a similar spectral model. However, this source is also highly absorbed ($N_{\text{H}} \sim 8 \times 10^{22}$ cm $^{-2}$) making detection of a soft thermal component difficult. Its spectrum is relatively soft ($\Gamma \sim 2.3$; Degenaar et al. 2012a), similarly to AX J1754.2–2754.

In addition, there are several LMXB transients which never become very bright and only reach peak X-ray luminosities similarly to the very faint persistent sources. For example, the best-fitting model for the *XMM-Newton* spectrum of the very faint LMXB XTE J1719–291, which most likely harbours an NS, was modelled with a blackbody component with a temperature of ~ 0.3 keV combined with a power law with a photon index of $\Gamma \sim 1.7$. The source has a rather low column density, $N_{\text{H}} \sim 3 \times 10^{21}$ cm $^{-2}$ (Armas Padilla et al. 2011) and the addition of a soft thermal component to the fit model is statistically required, which contributes ~ 30 per cent to the 0.5–10 keV source flux. The 2–10 keV luminosity of the source during this *XMM-Newton* observation was 1.3×10^{34} erg s $^{-1}$ which is very similar to that of 1RXS J171824.2–402934 and 1RXH J173523.7–354013. Similarly, the transient NS LMXB

Swift J185003.2–005627 displayed a 0.5–10 keV luminosity of $\sim 3 \times 10^{35} \text{ erg s}^{-1}$ in its 2011 outburst. The best description for the *Swift* spectra was also with a two-component model with similar parameter values, and the thermal component contributed ~ 45 – 65 per cent to the total 0.5–10 keV source unabsorbed flux (Degenaar et al. 2012b).

From the above, it is clear that our understanding of the X-ray spectra of VFXBs is severely limited and hampered by the lack of sources in combination with the sometimes large absorption to the known sources. It seems that at the lowest luminosities (a few times $10^{34} \text{ erg s}^{-1}$) definitely a soft component (with a low kT of ~ 0.3 – 0.4 keV) is needed and that the power-law component is rather hard (photon index of 1.4–1.6). However, at luminosities of $10^{35} \text{ erg s}^{-1}$ or higher, the spectra either do not require a soft component at similar strength as seen for the fainter sources (e.g. in AX J1754.2–2754) or a rather strong soft component could be clearly detected as well (e.g. Swift J185003.2–005627; albeit with relatively high temperatures of 0.7 keV). The nature of this thermal component is not clear. However, considering that most of the sources harbour NS accretors, a plausible origin for this component is the NS surface or perhaps the boundary layer (if present). Low-level accretion on to the surface of an NS can indeed produce a blackbody like spectrum (Zampieri et al. 1995). Still, a disc origin cannot be ruled out since it was also possible to fit the data with a multicolour disc blackbody. Moreover, it is not clear that the soft component which can be detected in the different sources is always coming from the same region: it might be possible that in some sources we see the surface/boundary layer of the NS but in others we see emission from the disc.

Despite that a soft component is not needed in the spectra of all known sources that have $L_X \sim 10^{35} \text{ erg s}^{-1}$, the spectra of those sources are still remarkably soft compared to what is typically seen for sources at higher L_X (i.e. $10^{36} \text{ erg s}^{-1}$, with usually $\Gamma \lesssim 2$). It is unclear if all the softening can be explained by the introduction of a thermal soft component (e.g. as seen for Swift J185003.2–005627) since this is not required by the data of AX J1754.2–2754 and will only contribute at most 10–20 per cent to the 0.5–10 keV flux (see Table 1). Therefore, quite likely in a number of sources the soft spectra at $\sim 10^{35} \text{ erg s}^{-1}$ might be intrinsic to the power-law component. This is similar to what has been seen for bright transients which decay below a luminosity of $10^{36} \text{ erg s}^{-1}$ as well as for several transient VFXBs (Armas Padilla et al. 2011, 2013): their spectra become softer as their X-ray luminosities decrease. The fact that at the same low X-ray luminosities similar soft X-ray spectra are seen in persistent sources and in transient sources might suggest that both types of systems have similar accretion geometries in the luminosity regime 10^{35} – $10^{36} \text{ erg s}^{-1}$. Such softening of the power-law component is expected in ADAF- or RIAF-like accretion flows (see Armas Padilla et al. 2013, for a discussion).

What happens below a luminosity of $10^{35} \text{ erg s}^{-1}$ is not clear. The presence (in two of our sources) of a soft thermal component at a luminosity close to $10^{34} \text{ erg s}^{-1}$ causes the spectra of those sources to be as soft as observed. In fact, their power-law component seems to be rather hard with a photon index of ~ 1.5 . It is unclear if this power-law component is related to the one seen at higher luminosities (which would indicate that it becomes harder again at the lowest observed luminosities if indeed the softening from $10^{36} \text{ erg s}^{-1}$ down to $10^{35} \text{ erg s}^{-1}$ can be ascribed to changes in the power-law component) or that it is due to a different phenomena (in which case the process which produces the power-law component seen at $> 10^{35} \text{ erg s}^{-1}$ must have disappeared and must be replaced by a different process which also produces a power-law shape spectrum).

Therefore, currently it is unclear how the lowest luminosity sources fit in the overall picture of accreting X-ray binaries. More sources in this luminosity range have to be studied using very sensitive satellites like *XMM-Newton*. In particular, those sources which move (frequently) through the luminosity range 10^{34} – $10^{35} \text{ erg s}^{-1}$, such as the transient systems or highly variable systems.

The spectral characteristics of 1RXS J171824.2–402934 and 1RXH J173523.7–354013 are similar to some of the transient NS LMXBs in their quiescence state, especially those who have L_X between 10^{33} and $10^{34} \text{ erg s}^{-1}$. Also for those sources, their X-ray spectra can be described using a two-component model consisting of a thermal part (fitted usually with a blackbody model or an NS atmosphere model) and a non-thermal part (usually fitted with a power-law model). Remarkably, the fit parameters obtained using such a model are very similar to what we have obtained for 1RXS J171824.2–402934 and 1RXH J173523.7–354013: a blackbody temperature of 0.2–0.3 keV and a photon index of ~ 1.5 (albeit that this is often not well constrained due to the low quality of the data) (e.g. Rutledge et al. 1999, 2002; Wijnands et al. 2002, 2004; Jonker et al. 2003; Cackett et al. 2011; Degenaar & Wijnands 2012). In this respect, it is interesting to note that when the thermal component in quiescent systems are fitted with a blackbody spectrum, small emitting radii are obtained (too small to be consistent with the expected radii of NS), similarly to what we observe for 1RXS J171824.2–402934 and 1RXH J173523.7–354013 (see Table 2). To explain those small radii in the quiescent systems, it has been argued that a blackbody model is not the correct model to use to fit the thermal component, but instead a neutron-star atmosphere model would be more appropriate (e.g. Brown, Bildsten & Rutledge 1998). Using such models, more realistic NS radii are indeed obtained (e.g. Rutledge et al. 1999, 2000). Applying such models to our targets also result in larger inferred radii (~ 10 km) but likely such models cannot be applied to our targets because they are still accreting. More appropriate models (like the one of Zampieri et al. 1995; Soria et al. 2011) have to be used for our targets, but it goes beyond the scope of this paper to discuss those models in detail.

The interpretation of the non-thermal component remains unclear (see Campana 2009; Degenaar & Wijnands 2012, and references therein). The similarity between these quiescent systems and our persistent accreting sources at a few times $10^{34} \text{ erg s}^{-1}$ could point that accretion might still be going on in quiescence for at least some of those sources which have quiescent luminosities of 10^{33} – $10^{34} \text{ erg s}^{-1}$. For systems which are fainter, this cannot be concluded because often either the thermal component is not present and only the power-law component (which often appears to be softer with a photon index of ~ 2 ; albeit again with large error bars) or only the soft component is seen with hardly any or no detectable contribution by a power-law component. In those latter systems, we could indeed observe the cooling of the NS. The physical process behind the fully non-thermally dominated quiescent spectra of a growing fraction of the quiescent systems is not understood.

ACKNOWLEDGEMENTS

MAP acknowledges the hospitality of the University of Michigan, where part of this work was carried out. We thank Alesandro Patruno and Lucy Heil for their useful comments on a previous version of this paper. This work made use of data from the *XMM-Newton* public data archive. ND is supported by NASA through Hubble Postdoctoral Fellowship grant number HST-HF-51287.01-A from the Space Telescope Science Institute (STScI). RW and MAP are

supported by an European Research Council starting grant awarded to RW.

REFERENCES

- Armas Padilla M., Degenaar N., Patruno A., Russell D. M., Linares M., Maccarone T. J., Homan J., Wijnands R., 2011, *MNRAS*, 417, 659
- Armas Padilla M., Degenaar N., Russell D. M., Wijnands R., 2013, *MNRAS*, 428, 3083
- Arnaud K. A., 1996, in Jacoby G. H., Barnes J., eds, *ASP Conf. Ser. Vol. 101, XSPEC: The First Ten Years*. Astron. Soc. Pac., San Francisco, p. 17
- Bassa C. et al., 2008, *Astron. Telegram*, 1575
- Brown E. F., Bildsten L., Rutledge R. E., 1998, *ApJ*, 504, L95
- Cackett E. M., Fridriksson J. K., Homan J., Miller J. M., Wijnands R., 2011, *MNRAS*, 414, 3006
- Campana S., 2009, *ApJ*, 699, 1144
- Chelovekov I. V., Grebenev S. A., 2007, *Astron. Lett.*, 33, 807
- Cooper R. L., Narayan R., 2007, *ApJ*, 661, 468
- Degenaar N., Wijnands R., 2009, *A&A*, 495, 547
- Degenaar N., Wijnands R., 2010, *A&A*, 524, A69
- Degenaar N., Wijnands R., 2012, *MNRAS*, 422, 581
- Degenaar N. et al., 2010, *MNRAS*, 404, 1591
- Degenaar N., Wijnands R., Kaur R., 2011, *MNRAS*, 414, L104
- Degenaar N. et al., 2012a, *A&A*, 540, A22
- Degenaar N., Linares M., Altamirano D., Wijnands R., 2012b, *ApJ*, 759, 8
- Degenaar N., Altamirano D., Wijnands R., 2012c, *Astron. Telegram*, 4219
- Del Santo M., Sidoli L., Mereghetti S., Bazzano A., Tarana A., Ubertini P., 2007a, *A&A*, 468, L17
- Del Santo M., Romano P., Sidoli L., Bazzano A., 2007b, *Astron. Telegram*, 1143
- Del Santo M., Sidoli L., Romano P., Bazzano A., Tarana A., Ubertini P., Federici M., Mereghetti S., 2008, in Bandyopadhyay R. M., Wachter S., Gelino D., Gelino C. R., eds, *AIP Conf. Ser. Vol. 1010, Sub-luminous X-ray Bursters Unveiled with INTEGRAL*. Am. Inst. Phys., New York, p. 162
- Done C., Diaz Trigo M., 2010, *MNRAS*, 407, 2287
- in't Zand J. J. M., Cornelisse R., Méndez M., 2005, *A&A*, 440, 287
- in't Zand J. J. M., Jonker P. G., Markwardt C. B., 2007, *A&A*, 465, 953
- in't Zand J. J. M., Jonker P. G., Bassa C. G., Markwardt C. B., Levine A. M., 2009, *A&A*, 506, 857
- Israel G. L. et al., 2008, *Astron. Telegram*, 1528
- Jonker P. G., Keek L., 2008, *Astron. Telegram*, 1643
- Jonker P. G., Méndez M., Nelemans G., Wijnands R., van der Klis M., 2003, *MNRAS*, 341, 823
- Kapteijn R. G., in't Zand J. J. M., Kuulkers E., Verbunt F., Heise J., Cornelisse R., 2000, *A&A*, 358, L71
- King A. R., 2000, *MNRAS*, 315, L33
- King A. R., Wijnands R., 2006, *MNRAS*, 366, L31
- Krivonos R., Revnivtsev M., Lutovinov A., Sazonov S., Churazov E., Sunyaev R., 2007, *A&A*, 475, 775
- Kuulkers E., den Hartog P. R., in't Zand J. J. M., Verbunt F. W. M., Harris W. E., Cocchi M., 2003, *A&A*, 399, 663
- Maccarone T. J., Patruno A., 2013, *MNRAS*, 428, 1335
- Maccarone T. J. et al., 2012, *Astron. Telegram*, 4109, 1
- Makishima K., Maejima Y., Mitsuda K., Bradt H. V., Remillard R. A., Tuohy I. R., Hoshi R., Nakagawa M., 1986, *ApJ*, 308, 635
- Nelemans G., Jonker P. G., 2010, *New Astron. Rev.*, 54, 87
- Nelson L. A., Rappaport S. A., Joss P. C., 1986, *ApJ*, 304, 231
- Patruno A., 2010, *Proc. High Time Resolution Astrophysics. The Era of Extremely Large Telescopes (HTRA-IV)* (<http://pos.sissa.it/cgi-bin/reader/conf.cgi?confid=108>)
- Peng F., Brown E. F., Truran J. W., 2007, *ApJ*, 654, 1022
- Rutledge R. E., Bildsten L., Brown E. F., Pavlov G. G., Zavlin V. E., 1999, *ApJ*, 514, 945
- Rutledge R. E., Bildsten L., Brown E. F., Pavlov G. G., Zavlin V. E., 2000, *ApJ*, 529, 985
- Rutledge R. E., Bildsten L., Brown E. F., Pavlov G. G., Zavlin V. E., 2002, *ApJ*, 577, 346
- Sakano M., Koyama K., Murakami H., Maeda Y., Yamauchi S., 2002, *ApJS*, 138, 19
- Sidoli L., Mereghetti S., 2003, *Astron. Telegram*, 147, 1
- Soria R., Zampieri L., Zane S., Wu K., 2011, *MNRAS*, 410, 1886
- Strüder L. et al., 2001, *A&A*, 365, L18
- Turner M. J. L. et al., 2001, *A&A*, 365, L27
- Verner D. A., Ferland G. J., Korista K. T., Yakovlev D. G., 1996, *ApJ*, 465, 487
- Wijnands R., 2008, in Bandyopadhyay R. M., Wachter S., Gelino D., Gelino C. R., eds, *AIP Conf. Ser. Vol. 1010, Enigmatic Sub-luminous Accreting Neutron Stars in our Galaxy*. Am. Inst. Phys., New York, p. 382
- Wijnands R., Guainazzi M., van der Klis M., Méndez M., 2002, *ApJ*, 573, L45
- Wijnands R., Homan J., Miller J. M., Lewin W. H. G., 2004, *ApJ*, 606, L61
- Wijnands R. et al., 2006, *A&A*, 449, 1117
- Wilms J., Allen A., McCray R., 2000, *ApJ*, 542, 914
- Zampieri L., Turolla R., Zane S., Treves A., 1995, *ApJ*, 439, 849
- Zdziarski A. A., Johnson W. N., Magdziarz P., 1996, *MNRAS*, 283, 193
- Życki P. T., Done C., Smith D. A., 1999, *MNRAS*, 309, 561

This paper has been typeset from a $\text{\TeX}/\text{\LaTeX}$ file prepared by the author.